Sliding-mode-based Relative Pose Synchronous Control in Space Autonomous Rendezvous

Wenhua Cheng, Yasheng Zhang, and Hong Yao
Equipment Academy, Beijing, PR China
Email: {cheng007wenhua, lizhizys, momoridy}@163.com

***Abstract*—With the development of space exploration technology and space commercial activities, the number of spacecraft in space is sharp increasing, space resources and environment is facing enormous challenges. Space Autonomous Rendezvous (SAR) is a multidisciplinary complex systems engineering, and has high demands on the precision, reliability, security, and other state constraints. In this paper, the pose synchronization control characteristics are analyzed. Then, the sliding mode surface function and control law are designed, and the feasibilities are proved. After that, via the simulation, pose synchronization control can be achieved with the sliding mode control law. Finally, the control parameter impact on system is analyzed and the result will help to the control system design.**

***Index Terms*—space autonomous rendezvous, synchronous control, sliding-mode control, relative pose**

I. Introduction

With the development of space exploration technology and space commercial activities, the number of spacecraft in space is sharp increasing, space resources and environment is facing enormous challenges. Space Autonomous Rendezvous, related to proximity operations between service spacecraft and target spacecraft, is not only a multi-dimensional state control problem including relative position relative attitude, but also a multidisciplinary complex systems engineering which contains mathematics, physics, mechanics and other basic disciplines, and combined with control, computer simulation and other technical disciplines. Space Autonomous Rendezvous requires that the autonomous rendezvous task is still able to carry out without relying on ground support especially in the blind spot of ground control stations. Thus, the precision, reliability, security, and other state constraints are facing with very high demands [1]-[4].

For spacecraft orbit and attitude control problem, the traditional method is to put it into separated orbital and attitude control. As humans' demand for space continues increasing, space missions become more and more complex. Thus, the complex missions require that relative pose can simultaneously and quickly meet the control requirements. The traditional method is no longer able to meet the needs of these tasks. In contrast, the pose synchronous control takes position and attitude as a whole, adopts unified control strategy, from the perspective of the global system, achieves position and attitude synchronous control, and improves the control accuracy and performance essentially.

In fact, each spacecraft has a strong coupling of position and attitude. Thus, there are many researches on synchronous control. Misra and Sanyal [5] make a study on the relationship between the motion and angular motion in asteroid mission. The simulation results show that the position and the attitude have a strong coupling, especially in approach phase. Pan *et al.* [6], [7] propose a matrix nonlinear controller to determine the relative velocity and angular velocity. Single *et al.* [8] propose a output feedback controller for spacecraft rendezvous and docking, and analyze the error. Komanduri *et al.* [9] design a linear quadratic controller to track the relative position and attitude of non-cooperative spacecraft. Lee *et al.* [10] design a guidance and control system for the final approach, and simulation results show the performance is well. In [11], the dynamics and control problem of final approach between the servicer spacecraft and target spacecraft are studied. A variety of control laws are proposed based on the detail analysis of relative position and attitude in [12]. The coupling effect of orbit and attitude is illustrated quantitatively in [13] based on dual quaternion, same studied in [14]. Results show that synchronous control not only meets the accuracy requirement, but also saves the cost.

II. Characteristics of Pose Synchronous Control

During Space Autonomous Rendezvous, relative position and attitude between service spacecraft and target spacecraft is changing constantly, especially in close range rendezvous and final approach which requires that the relative position and relative attitude meet the requirements at the same time. Therefore, the pose needs to be adjusted quickly. On the other hand, due to the different control actuator installation styles and errors, the position and attitude will be coupled, pose synchronous control is needed. Moreover, even in far range rendezvous, the spacecraft needs to constantly modulate the attitude in order to achieve the desired thrust. Pose synchronous control can solve the above problems, and has the following characteristics:

(1) High precision: Compared to the traditional control strategies, pose synchronization control can solve the

Manuscript received August 1, 2015; accepted November 21, 2015.

doi: 10.18178/joace.4.5.375-379

problems that position control and attitude control cannot meet the high accuracy requirements at the same time, and can achieve good balance between position control and attitude control with high accuracy;

(2) High efficiency: the traditional pose control separates the position control and attitude control. Thus, two independent control systems need to be designed and to be balanced with each other. But, using pose synchronous control, which takes the position and attitude control as a whole , can essentially save the design costs and improve control efficiency;

(3) High mobility: During the maneuver, the space craft often makes the orbital maneuvering before attitude modulation. Synchronous control makes the position and attitude modulated at the same time based on the desired pose information. This integrity makes the spacecraft mobility stronger, especially in small relative distance where the advantage is more obvious.

In summary, compared to traditional control strategy, pose synchronization control not only improves the control efficiency and accuracy of spacecraft, but also enhances spacecraft mobility. Fig. 1 illustrates the traditional separate control and synchronous control.

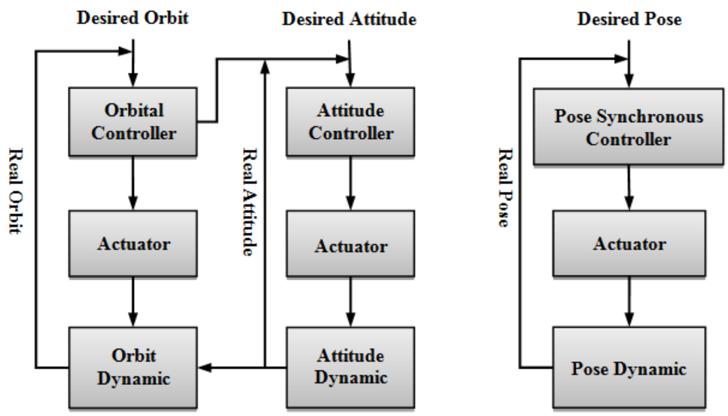

(a) The Traditional Separate Control *(b)* the Synchronous Control

Figure 1. The traditional separated control and the synchronous control

III. Problem Definition

A. Relative Pose Dynamic Model

Relative pose dynamic model as follows [15]:

$$\ddot{\boldsymbol{R}}\big|_S = \frac{\mu}{R_S{}^3}\left(\frac{3x}{R_S}\boldsymbol{R}_S|_S\right) - 2\boldsymbol{\omega}_0 \times \dot{\boldsymbol{R}}\big|_S - \dot{\boldsymbol{\omega}}_0|_S \times \boldsymbol{R} - \boldsymbol{\omega}_0 \times (\boldsymbol{\omega}_0 \times \boldsymbol{R}) - \boldsymbol{f}_S$$
$$\dot{\boldsymbol{q}} = \frac{1}{2}\begin{bmatrix} \boldsymbol{\omega} & -[\boldsymbol{\omega}\times] \\ \boldsymbol{0} & -\boldsymbol{\omega}^T \end{bmatrix}\boldsymbol{q}$$
$$\dot{\boldsymbol{\omega}}|_S = \boldsymbol{D}(\boldsymbol{q})\{\boldsymbol{I}_T^{-1}[-(\boldsymbol{\omega}_S + \boldsymbol{\omega}) \times \boldsymbol{I}_T(\boldsymbol{\omega}_S + \boldsymbol{\omega})]\} - \boldsymbol{I}_S^{-1}(\boldsymbol{T}_S - \boldsymbol{\omega}_S \times \boldsymbol{I}_S\boldsymbol{\omega}_S) \tag{1}$$

If

$$\boldsymbol{D} = \boldsymbol{D}(\boldsymbol{q})\{\boldsymbol{I}_T^{-1}[-(\boldsymbol{\omega}_S + \boldsymbol{\omega}) \times \boldsymbol{I}_T(\boldsymbol{\omega}_S + \boldsymbol{\omega})]\} + \boldsymbol{I}_S^{-1}(\boldsymbol{\omega}_S \times \boldsymbol{I}_S\boldsymbol{\omega}_S) \tag{2}$$

Then

$$\dot{\boldsymbol{\omega}} = \boldsymbol{D} - \boldsymbol{I}_S^{-1}\boldsymbol{T}_S \tag{3}$$

Define state variables as

$$\boldsymbol{X} = [\boldsymbol{R}^T, \boldsymbol{q}^T]^T$$

Thus, the relative pose dynamic model can be illustrated as

$$\ddot{\boldsymbol{X}} = \boldsymbol{A}\dot{\boldsymbol{X}} + \boldsymbol{B}\boldsymbol{X} + \boldsymbol{C}\boldsymbol{U} \tag{4}$$

where

$$\boldsymbol{A} = \begin{bmatrix} \boldsymbol{A}_1 & \boldsymbol{0} \\ \boldsymbol{0} & \boldsymbol{A}_2 \end{bmatrix},\ \boldsymbol{B} = \begin{bmatrix} \boldsymbol{B}_1 & \boldsymbol{0} \\ \boldsymbol{0} & \boldsymbol{B}_2 \end{bmatrix},\ \boldsymbol{C} = \begin{bmatrix} \boldsymbol{C}_1 & \boldsymbol{0} \\ \boldsymbol{0} & \boldsymbol{C}_2 \end{bmatrix},\ \boldsymbol{U} = \begin{bmatrix} \boldsymbol{f}_S \\ \boldsymbol{T}_S \end{bmatrix}$$

$$\boldsymbol{A}_1 = \begin{bmatrix} 0 & 2\dot{\theta}_S & 0 \\ -2\dot{\theta}_S & 0 & 0 \\ 0 & 0 & 0 \end{bmatrix},\ \boldsymbol{A}_2 = \frac{1}{2}\begin{bmatrix} \omega & -[\omega\times] \\ 0 & -\omega^T \end{bmatrix}$$

$$\boldsymbol{B}_1 = \begin{bmatrix} \dot{\theta}_S^2 + \frac{2\mu}{R_S{}^3} & \ddot{\theta}_S & 0 \\ -\ddot{\theta}_S & \dot{\theta}_S^2 - \frac{\mu}{R_S{}^3} & 0 \\ 0 & 0 & -\frac{\mu}{R_S{}^3} \end{bmatrix},\ \boldsymbol{B}_2 = \frac{1}{2}\begin{bmatrix} D & -[D\times] \\ 0 & -D^T \end{bmatrix}$$

$$\boldsymbol{C}_1 = \begin{bmatrix} -1 & 0 & 0 \\ 0 & -1 & 0 \\ 0 & 0 & -1 \end{bmatrix},\ \boldsymbol{C}_2 = -\frac{1}{2}\begin{bmatrix} q_0 & -q_3 & q_2 \\ q_3 & q_0 & -q_1 \\ -q_2 & q_1 & q_0 \\ -q_1 & -q_2 & -q_3 \end{bmatrix} I_S^{-1}$$

So, state error can be defined as

$$\boldsymbol{X}_e = \boldsymbol{X} - \boldsymbol{X}_f \tag{5}$$

where $\boldsymbol{X}_f$ denotes desired pose state.And

$$\dot{\boldsymbol{X}}_e = \dot{\boldsymbol{X}} - \dot{\boldsymbol{X}}_f, \ddot{\boldsymbol{X}}_e = \ddot{\boldsymbol{X}} - \ddot{\boldsymbol{X}}_f$$

B. Sliding Mode Surface Function Design

Design sliding mode surface function as

$$\boldsymbol{s} = \dot{\boldsymbol{X}}_e + \boldsymbol{K}\boldsymbol{X}_e \tag{6}$$

where $\boldsymbol{K} \in \mathbb{R}^{7\times 7}$.

When system is controlled to the sliding mode surface, it yields

$$\boldsymbol{s} = \dot{\boldsymbol{X}}_e + \boldsymbol{K}\boldsymbol{X}_e = \boldsymbol{0}$$

i.e.

$$\dot{\boldsymbol{X}}_e = -\boldsymbol{K}\boldsymbol{X}_e \tag{7}$$

In order to validate stability of function, the candidate Lyapunov function is defined as

$$V_1 = \frac{1}{2}\boldsymbol{X_e}^T\boldsymbol{X_e} \tag{8}$$

Computing the first-order derivative of V_1 yields

$$\dot{V}_1 = \boldsymbol{X_e}^T\dot{\boldsymbol{X}}_e = -\boldsymbol{X_e}^T\boldsymbol{K}\boldsymbol{X_e} \leq \boldsymbol{0} \tag{9}$$

According the Lyapunov stability theory [16], the surface function is asymptotic convergence. Thus, $\lim_{t\to\infty}\boldsymbol{X_e} = \boldsymbol{0}$ and $\lim_{t\to\infty}\boldsymbol{X} = \boldsymbol{X_f}$.

C. Feedback Control Law Design

Design feedback control law as follows:

$$\dot{\boldsymbol{s}} = -\boldsymbol{\varepsilon} sgn\boldsymbol{s} - \boldsymbol{K_1}\boldsymbol{s} \tag{10}$$

where $\boldsymbol{\varepsilon}$, $\boldsymbol{K_1} \in \mathbb{R}^{7\times7}$.

Computing the first-order derivative of (6) yields

$$\dot{\boldsymbol{s}} = \ddot{\boldsymbol{X}}_e + \boldsymbol{K}\dot{\boldsymbol{X}}_e \tag{11}$$

Combining (10) and (11) yields

$$\ddot{\boldsymbol{X}}_e + (\boldsymbol{K} + \boldsymbol{K_1})\dot{\boldsymbol{X}}_e + \boldsymbol{K}\boldsymbol{K_1}\boldsymbol{X_e} + \boldsymbol{\varepsilon} sgn\boldsymbol{s} = \boldsymbol{0} \tag{12}$$

Substituting $\ddot{\boldsymbol{X}}_e$ into (12) yields

$$\boldsymbol{A}\dot{\boldsymbol{X}} + \boldsymbol{B}\boldsymbol{X} + \boldsymbol{C}\boldsymbol{U} - \ddot{\boldsymbol{X}}_f + (\boldsymbol{K} + \boldsymbol{K_1})\dot{\boldsymbol{X}}_e + \boldsymbol{K}\boldsymbol{K_1}\boldsymbol{X_e} + \boldsymbol{\varepsilon} sgn\boldsymbol{s} = \boldsymbol{0} \tag{13}$$

Hence the control law can be illustrated as

$$\boldsymbol{U} = \boldsymbol{C}^{-1}(\ddot{\boldsymbol{X}}_f - \boldsymbol{A}\dot{\boldsymbol{X}} - \boldsymbol{B}\boldsymbol{X} - (\boldsymbol{K} + \boldsymbol{K_1})\dot{\boldsymbol{X}}_e - \boldsymbol{K}\boldsymbol{K_1}\boldsymbol{X_e} - \boldsymbol{\varepsilon} sgn\boldsymbol{s}) \tag{14}$$

The candidate Lyapunov function is defined as

$$V_2 = \frac{1}{2}\boldsymbol{s}^T\boldsymbol{s} \tag{15}$$

Computing the first-order derivative of V_2 yields

$$\dot{V}_2 = \boldsymbol{s}^T\dot{\boldsymbol{s}} = \boldsymbol{s}^T(\ddot{\boldsymbol{X}}_e + \boldsymbol{K}\dot{\boldsymbol{X}}_e) = \boldsymbol{s}^T(-\boldsymbol{K_1}\dot{\boldsymbol{X}}_e - \boldsymbol{K}\boldsymbol{K_1}\boldsymbol{X_e} - \boldsymbol{\varepsilon} sgn\boldsymbol{s}) = -\boldsymbol{s}^T\boldsymbol{K_1}\boldsymbol{s} - \boldsymbol{s}^T\boldsymbol{\varepsilon} sgn\boldsymbol{s} \leq -\boldsymbol{s}^T\boldsymbol{K_1}\boldsymbol{s} \leq \boldsymbol{0} \tag{16}$$

According the Lyapunov stability theory, the system state is asymptotic convergence via the control law.

IV. Simulation and Result

In this section, different simulation cases are presented to illustrate and validate the theoretical concepts introduced above. Initialization conditions as follows.

Initial parameters	
Servicer orbit parameters	$\{7000km \quad 0.1 \quad 60° \quad 100° \quad 30° \quad 0s\}$
Inertia matrix	$\boldsymbol{I_S} = \boldsymbol{I_T} = diag[100 \quad 110 \quad 120](kgm^2)$
Initial relative position	$\boldsymbol{R}_0 = [300 \quad -400 \quad 500]^T(m)$
Initial relative attitude	$\boldsymbol{q}_0 = [-0.5 \quad -0.5 \quad 0.5 \quad -0.5]^T$
Initial relative angular velocity	$\boldsymbol{\omega}_0 = [0.01 \quad 0.01 \quad 0.01]^T(rad/s)$
Desired relative pose	$\boldsymbol{X_f} = [0 \quad 0 \quad 0 \quad 1 \quad 0 \quad 0 \quad 0]^T$
Simulation parameters	
Simulation time	$t = 1000s$
Simulation step size	$h = 0.01s$
Control parameters	
Parameter K	$\boldsymbol{K} = diag[0.02 \quad 0.02 \quad 0.02 \quad 0.02 \quad 0.02 \quad 0.02 \quad 0.02]$
Parameter K_1	$\boldsymbol{K_1} = diag[0.01 \quad 0.01 \quad 0.01 \quad 0.01 \quad 0.01 \quad 0.01 \quad 0.01]$
Parameter ε	$\boldsymbol{\varepsilon} = diag[4 \quad 4 \quad 4 \quad 4 \quad 4 \quad 4 \quad 4] \times 10^{-6}$

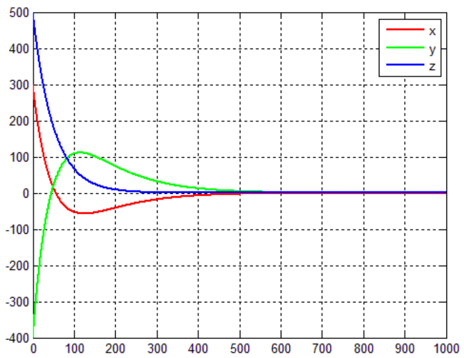

Figure 2. Relative position curve

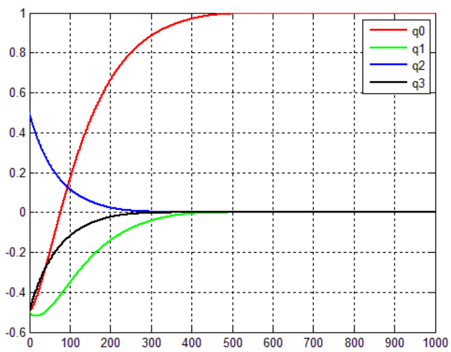

Figure 3. Relative attitude curve

The simulation results are illustrated in Fig. 2 and Fig. 3. In Fig. 2 and Fig. 3, relative pose converges on desired pose at time 500s via control. Thus, the effectiveness of control law is validated. In order to make a contribution to the design of control system, the impact of the control parameters are analyzed.

A. Parameter K

Parameter $\boldsymbol{K}$ is given as follows:

$$\boldsymbol{K} = \text{diag}[0.01 \quad 0.01 \quad 0.01 \quad 0.01 \quad 0.01 \quad 0.01 \quad 0.01]$$

$$\boldsymbol{K} = \text{diag}[0.04 \quad 0.04 \quad 0.04 \quad 0.04 \quad 0.04 \quad 0.04 \quad 0.04]$$

Other conditions are same as above. The simulation results are illustrated in Fig. 4.

Comparing Fig. 4 and Fig. 2 yields that when K=0.01, 0.02 and 0.04, system state converges on desired pose at time 800s, 500s and 300s. Thus, parameter $\boldsymbol{K}$ can influence system convergence velocity. The larger K is, the faster system converges to desired state.

B. Parameter K_1

Parameter $\boldsymbol{K_1}$ is given as follows:

$$\boldsymbol{K_1} = \text{diag}[0.005 \quad 0.005 \quad 0.005 \quad 0.005 \quad 0.005 \quad 0.005 \quad 0.005]$$

$$\boldsymbol{K_1} = \text{diag}[0.02 \quad 0.02 \quad 0.02 \quad 0.02 \quad 0.02 \quad 0.02 \quad 0.02]$$

Other conditions are same as above. The simulation results are illustrated in Fig. 5.

Comparing Fig. 5 and Fig. 2 yields that Parameter $\boldsymbol{K_1}$ is same as the parameter $\boldsymbol{K}$, which influences the system convergence velocity.

C. Parameter ε

Parameter ε is given as follows:

$$\boldsymbol{\varepsilon} = \mathrm{diag}[4 \quad 4 \quad 4 \quad 4 \quad 4 \quad 4 \quad 4] \times 10^{-4}$$

$$\boldsymbol{\varepsilon} = \mathrm{diag}[4 \quad 4 \quad 4 \quad 4 \quad 4 \quad 4 \quad 4] \times 10^{-2}$$

Other conditions are same as above. The simulation results are illustrated in Fig. 6.

In Fig. 6, parameter ε can also influence system convergence velocity but not as strong as parameter $\boldsymbol{K}$ and $\boldsymbol{K_1}$.

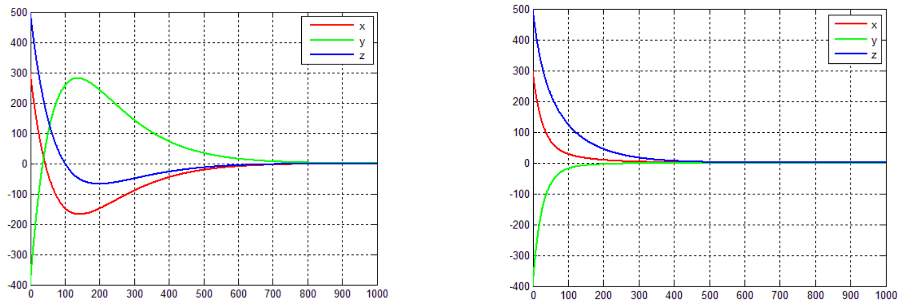

(a) *K*=0.01 (b) *K*=0.04

Figure 4. Variable parameter K and its' impact

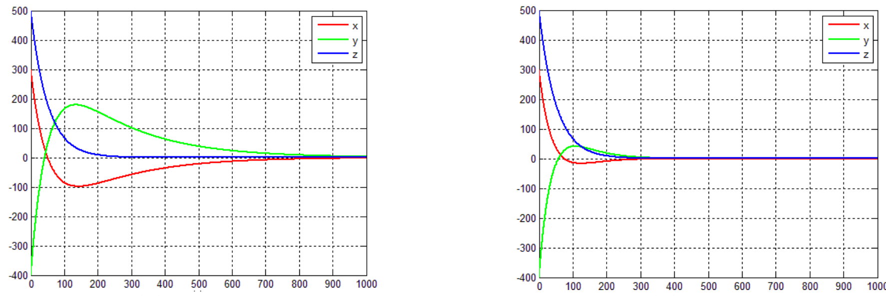

(a) K_1=0.005 (b) K_1=0.02

Figure 5. Variable parameter K_1 and its' impact

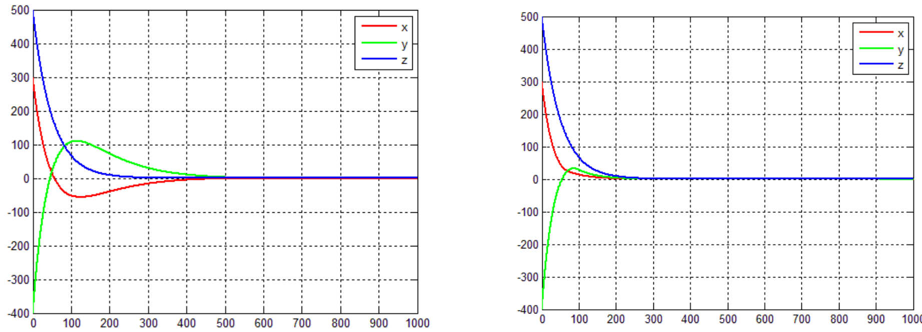

(a) $\boldsymbol{\varepsilon}$ =0.0004 (b) $\boldsymbol{\varepsilon}$ =0.04

Figure 6. Variable parameter ε and its' impact

V. CONCLUSION

In this paper, the pose synchronization control characteristics are analyzed. Then, the sliding mode surface function and control law are designed, and the feasibilities are proved. After that, via the simulation, pose synchronization control can be achieved with the sliding mode control law. Finally, the control parameter impact on system is analyzed and the result will help to the control system design.

ACKNOWLEDGEMENT

Research for this paper is supported by the National Natural Science Foundation of China, grant 61304228.

REFERENCE

[1] W. Fehse, *Automated Rendezvous and Docking of Spacecraft*, U.K.: Cambridge University Press, 2003.

[2] B. N. Zhang, *Spacecraft Rendezvous and Docking Missions Analysis and Design*, Beijing: Science Press, 2011.

[3] L. H. Liu, Y. H. Meng, and X. Y. An, *Spacecraft Relative Orbital Dynamic and Control*, Beijing: China Astronautics Press, 2013.

[4] L. P. Yang, Y. W. Zhu, and H. Huang, *Spacecraft Relative Motion Track Plan and Control*, Beijing: National Defense Industry Press, 2010.

[5] G. Misra and A.Sanyal, "Analysis of orbit-attitude coupling of spacecraft near small solar system bodies," in *Proc. AIAA Guidance, Navigation, and Control Conf.*, 2015.

[6] H. Z. Panand Vikram Kapila, "Adaptive nonlinear control for spacecraft formation flying with coupled translational and attitude

dynamics," in *Proc. 40th IEEE Conference on Decision and Control*, vol. 3, 2001.
[7] H. Wong, H. Z. Pan, and Vikram Kapila, "Output feedback control for spacecraft formation flying with coupled translation and attitude dynamics," in *Proc. American Control Conference*, 2005.
[8] S. Puneet, K. Subbarao, and J. L. Junkins, "Adaptive output feedback control for spacecraft rendezvous and docking under measurement uncertainty," *Journal of Guidance, Control, and Dynamics*, vol. 29, no. 4, pp. 892-902, 2006.
[9] A. S. Komanduri, *et al*. "Tracking controllers for position and attitude on the chaser spacecraft to rendezvous and dock/berthing with a non-cooperative spacecraft," in *Proc. 62nd International Astronautical Congress*, 2011.
[10] L. Holguin, S. P. Viswanathan, and A.Sanyal, "Guidance and control for spacecraft autonomous rendezvous and proximity maneuvers using a geometric mechanics framework," in *Proc. AIAA Guidance, Navigation, and Control Conf*., 2012.
[11] F. Wang, X. Q. Chen, and X. B. Cao, "The research of on-orbit parameters estimation for on-orbit-servicing spacecraft relative to out-of-control spacecraft," *Journal of Astronautics*, vol. 30, no. 4, pp. 1396-1403, 2009.
[12] W. Lu, Y. H. Geng, X. Q. Chen, *et al*. "Coupled control of relative position and attitude for on-orbit servicing spacecraft with respect to target," *Acta Aeronautica et Astronautica Sinica*, vol. 32, no. 5, pp. 857-865, 2011.
[13] J. Y. Wang, H. C. Liang, and Z. W. Sun,"Dual number-based relative coupled dynamics and control," *Journal of Astronautics*, vol. 7, pp. 1711-1717, 2010.
[14] Z. H. Peng, J. J. Mu, L. J. Zhang, *et al*. "Spacecraft attitude and orbital coupling dynamics and control based on dual quaternion," *Journal of Spacecraft TT&C Technology*, vol. 32, no. 6, pp. 549-554, 2013.
[15] D. Zhou, "Estimation of relative state between non-cooperative spacecraft based on stereo-vision," M.E. thesis, Harbin Institute of Technology, 2015.
[16] B. Liu and W. S. Tang, *Modern Control Theory*, Beijing: China Machine Press, 2006.

Wenhua Cheng received the B.E. degree in Flight Vehicle Design and Engineering from Harbin Institute of Technology, Harbin, China. He is currently working toward the M.E. in Space Mission Analysis and Design in the Department of Space Equipment, Equipment Academy, Beijing, China. His current research interests include Onboard Guidance, Navigation and Control, Space Autonomous Rendezvous, Relative Position and Attitude Estimation, Computer and Machine Vision.

Yasheng Zhang received the B.E. degree and the M.E. degree in Flight Vehicle Design from National University of Defense Technology, Changsha, China, and received the Ph.D. degree in Military Equipment from Equipment Academy, Beijing, China. She is currently the professor of Department of Space Equipment, Equipment Academy. Her areas of research interest include Space Mission Analysis and Design, Spacecraft Dynamics, Navigation and Control.

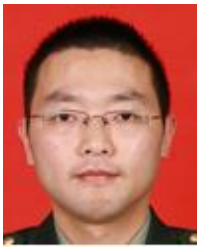

Hong Yao received the B.E. degree, the M.E. degree and the Ph.D. degree in Flight Vehicle Design from National University of Defense Technology, Changsha, China. He is currently the associate professor of Department of Space Equipment, Equipment Academy. His areas of research interest include Space Mission Analysis and Design, Spacecraft Formation Flying Dynamics, Navigation and Control.